ARTICLES
PUBLISHED ONLINE: 11 NOVEMBER 2012 | DOI: 10.1038/NPHYS2463
nature physics

Hyper-transport of light and stochastic acceleration by evolving disorder

Liad Levi, Yevgeny Krivolapov, Shmuel Fishman and Mordechai Segev*

In 1958, Philip Anderson argued that disorder can transform a conductor into an insulator, as multiple scattering from disorder brings transport to a complete halt. This concept, known as Anderson localization, has been tested in electronic, optical, acoustic and matter wave systems, which have all shown that disorder generally works to arrest transport. One major condition is common to all work on Anderson localization: for localization to take place, the underlying potential must be constant in time (frozen). Otherwise, if the disorder is dynamically evolving, localization breaks down and diffusive transport is expected to prevail. However, it seems natural to ask: can disorder increase the transport rate beyond diffusion, possibly even beyond ballistic transport? Here, we use a paraxial optical setting as a model system, and demonstrate experimentally and numerically that an evolving random potential gives rise to stochastic acceleration, which causes an initial wave packet to expand at a rate faster than ballistic, while its transverse momentum spectrum continuously expands. We discuss the universal aspects of the phenomenon relevant for all wave systems containing disorder.

Over the past 50 years, Anderson localization[1] has been studied in many experiments, in periodic systems containing disorder[2–4] as well as in fully random potentials[5–12]. These studies, and many more theoretical studies, addressed the regime where the disordered potential is frozen. Some researchers also explored transport in potentials that are random in space and also fluctuate in time[13]. However, only a small number of studies, all strictly theoretical, suggested hyper-transport: transport mechanisms through which the region within which a particle can be found expands faster than ballistic expansion[14–18]. A robust picture of such motion in terms of resonances between the particle and the potential was developed in ref. 14. Ten years later, ref. 15 addressed a similar setting in the framework of quantum mechanics. Assuming a spatially random potential fluctuating in time with a Gaussian white-noise spectrum, they suggested that the root-mean-square displacement of the particle grows with exponent 3/2 in time (rather than 1/2 for diffusion and 1 for ballistic transport). Later on, several theoretical studies identified hyper-transport of particles[16–18] for fluctuating potentials with correlated disorder (that is, when the bandwidth of the disorder is finite). However, thus far there has been no experimental evidence for hyper-transport by disorder. The experimental demonstration presented here is the first experimental proof that disorder can give rise to hyper-transport: transport at a rate faster than ballistic.

In the experiments presented here, we study the transport of waves in a paraxial optical system, which can be viewed as analogous to the transport in a quantum system[19–21]. In this setting, light propagating in a waveguide array exhibits evolution analogous to that of an electron in an atomic lattice[21]. Importantly, this system enables direct observation of the actual wave packets, which is a key aspect in unravelling the mechanisms underlying transport. Indeed, recent experiments in this photonic system investigated fundamental transport processes, such as Anderson localization in lattices[3,4,22], in quasicrystals[23,24] and near interfaces[25]. Likewise, analogous experiments on Anderson localization were demonstrated with matter waves in disordered optical potentials[8–11]. However, none of these experiments studied transport in the presence of disorder that also fluctuates during evolution. So far, all Anderson localization experiments in optics as well as in matter wave systems concentrated on the effects of frozen disorder on the transport of wave packets. On the other hand, some pioneering experiments in optics did demonstrate enhanced broadening due to the presence of disorder. One example is, Lévy flights—where in the ray-optics regime, light propagating in a disordered system performs an unusual random walk with a step length governed by the Lévy statistics, leading to superdiffusion[26]. Another example is light propagation through layered random media demonstrating crossover from localization to diffusion[27]. Another example is disorder-enhanced wave transport in quasicrystals[24]. However, in none of these has the transport rate ever exceeded the rate of ballistic transport.

Our experiments employ an optical beam propagating through a photonic medium containing spatial disorder that is also fluctuating during evolution. Let us first describe the effect on universal grounds, in real space and in momentum space. The hallmark of ballistic transport is that the expansion rate of a wave packet is proportional to time, while the width of its spectrum in momentum space remains constant with time. This latter feature indicates that the population of momentum constituents does not change during evolution: only their phases evolve, in proportion with time. In contrast to ballistic evolution, in our hyper-transport experiments, the wave packet expands at a rate much faster than ballistic, while at the same time its width in momentum space also expands markedly during propagation. More specifically, we study the evolution of a laser beam propagating through a photonic medium containing dynamically evolving disorder. Our photonic system is described by a two-dimensional time-dependent Schrödinger-type equation with a disordered potential; hence, the wave packet and its Fourier transform, which are both directly viewed in our experiments, are analogous to the probability amplitudes of finding a quantum particle or its momentum[27], respectively. Strictly within the domain of optics, the results described below are intuitive. However, this direct analogy to transport in quantum systems makes our findings relevant for very many wave systems containing disorder.

Physics Department and Solid State Institute, Technion, Haifa 32000, Israel. *e-mail: msegev@tx.technion.ac.il.

We work with a photonic medium, in the transverse localization scheme[3,19] described by the paraxial equation for monochromatic light,

$$i\frac{\partial\Psi}{\partial z}=\left[-\frac{1}{2k}\left(\frac{\partial^2}{\partial x^2}+\frac{\partial^2}{\partial y^2}\right)-\frac{k}{n_0}\Delta n(x,y,z)\right]\Psi\triangleq\hat{H}\Psi \qquad (1)$$

Here z is the evolution (propagation) coordinate, x and y are the transverse dimensions, Ψ is the slowly varying envelope of an optical field $E(\bar{r},t)=\mathrm{Re}[\Psi(x,y,z)e^{i(kz-\omega t)}]$ of frequency ω and wavenumber $k=2\pi n_0/\lambda$. In our experiments, $n_0=2.34$ is the bulk refractive index, $\lambda=0.514\,\mu$m is the vacuum wavelength and $\Delta n(x,y,z)\sim 10^{-4}$ is the local change in the refractive index. To stay within the paraxial limit, $|\Delta n|\ll n_0$, and all of its spatial variations, as well as the fine details of Ψ, are on a scale much larger than λ. Equation (1) has the form of the Schrödinger equation: the equivalence emerges when the role of time t is played by the propagation distance z, and $-\Delta n\rightarrow V$, the optical potential[19]. Hence, the evolution of a light beam behaves like the wave packet of a quantum particle in a two-dimensional potential but with the coordinate z replacing time. In this scheme, the transverse wavevector $\mathbf{k}_\perp=(k_x,k_y)$ of the optical wave packet is equivalent to the momentum $\mathbf{p}=(p_x,p_y)$ of a quantum particle. In the paraxial regime where equation (1) is valid, $k_\perp\ll k_z,k$. This scheme, first proposed in 1989 (ref. 19), was used in previous experiments in optics investigating Anderson localization[3,4,21–25]. As Anderson localization occurs only if the disorder is frozen in time, those experiments required considerable care to make the disorder in the system perfectly uniform along the direction of propagation (the z axis). In contradistinction, here we aim to study transport in a temporally fluctuating spatially disordered system; hence, we design our experiments such that we can control the rate of z-variation of the disordered potential as it varies randomly in z, as well as its statistical properties.

Figure 1 shows the experimental scheme described by equation (1). We use the optical induction technique[3,28–30] to transform an optical intensity pattern into a variation in the refractive index, $\Delta n(x,y,z)$. The refractive index structure is formed within a bulk dielectric strontium barium niobate crystal by making use of the photorefractive screening nonlinearity[31]. To make the disorder random in the x–y plane, and at the same time have it evolving in z in a controllable manner, we pass a ring of light through a diffuser placed in the Fourier plane of a lens. The resultant interference pattern is a speckled structure whose plane-wave constituents (spatial spectrum) associated with transverse wavevectors, $\mathbf{k}_\perp$, reside within a ring of radius $k_{\perp 0}$ and thickness δk (Fig. 1). When $\delta k=0$, all of the plane-wave components accumulate phase at the same rate as they evolve in z, because they all have the same propagation constant $k_z=\sqrt{k^2-k_{\perp 0}^2}$. The outcome is a propagation-invariant speckled pattern, giving rise to frozen disorder[3], as required for observing Anderson localization. However, when $\delta k\neq 0$, the plane-wave constituents comprising the speckled pattern possess different k_z values. Consequently, the speckled pattern evolves with z, which is transformed (through the induction technique) into a disordered refractive index pattern that also evolves randomly in z. For our present experiments, it is essential to create disorder while controlling the statistics in the x–y plane, and the rate of its random fluctuations in z. In the x–y plane, the mean distance between speckles is set by the radius of the ring in momentum space, $k_{\perp 0}$, whereas the rate of z-evolution is determined by the thickness of the ring, δk (Fig. 2f–h). For this setting, the characteristic distance for the z-evolution of $\Delta n(x,y,z)$ can be estimated from the beating rate (in z) created by the interference between the two extreme plane waves residing on the outer and inner radii or the momentum-space ring, corresponding to transverse wavenumbers $k_\perp=k_{\perp 0}\pm\delta k$. The beating rate yields a characteristic distance $z_0=2\pi k/k_{\perp 0}\delta k$ for the evolution of the disordered potential. The larger δk is, the smaller z_0, and the faster the variations in z are. In this fashion, we generate disorder while controlling both its spectrum and its rate of dynamic evolution.

With this system in hand, we study transport by launching a weak, narrow, probe beam and monitoring the intensity pattern exiting the medium containing the disorder (Fig. 1). The probe beam is weak such that it does not contribute to the induced refractive-index pattern. It is propagating linearly through the medium, undergoing multiple scattering events from the disorder in the refractive index, as described by equation (1). As for experiments on Anderson localization in optics[3], meaningful results are obtained by repeating the experiments multiple times with many realizations of the disorder (from the same distribution), and ensemble-averaging over the intensity patterns at the exit face of the disordered medium.

We now describe the experimental results. We begin with the two established cases: free (ballistic) diffraction, and then localization. Figure 2a shows the width and the intensity cross-section of the beam in the absence of any disorder, where the wave packet is allowed to freely diffract through the medium and experience ballistic transport. The width of the beam exiting the medium is $\sim$166 μm, which agrees well with the calculated value for ballistic expansion of a Gaussian beam with an initial full-width half-maximum of $\sim$15 μm in a medium with a bulk refractive index of 2.34. Next, we establish propagation-invariant disorder, and demonstrate Anderson localization. Figure 2b shows the ensemble-averaged (over 100 realization of disorder) intensity structure of the beam exiting the medium, after propagating through the z-invariant spatial disorder. As shown at the bottom of Fig. 2b, the beam is exponentially localized, thereby exhibiting Anderson localization. One particular realization of the spatial disorder (for which the localization occurs) is shown in Fig. 2e, and its spatial spectrum—shaped as a narrow ring in the transverse momentum space—is shown in Fig. 2f. The speckled structure of the disorder is virtually z-invariant, as the ring in Fig. 2f is of a very narrow thickness ($\delta k\rightarrow 0$). For this case of an Anderson-localized beam, the mean width (defined as in ref. 3) of the exiting beam is $\sim$103 μm (with standard deviation of 23 μm)—much smaller than the width of the freely diffracting beam of Fig. 2a. These results on the beam propagating through z-invariant disorder are very similar to those presented in ref. 3.

Having established the two extreme cases (no disorder, and propagation-invariant disorder), we now proceed to experiment with dynamically evolving (fluctuating) disorder, and examine how it affects the evolution of the (ensemble-average) beam when the rate of dynamic fluctuations is increased. Figure 2c,d show the ensemble-averaged intensity structure and its cross-section (averaged over 50 realization of the disorder) of the same initial wave packet after propagating in the presence of spatial disorder whose spatial spectra are shown in Fig. 2g,h, respectively. In these cases, the variations of Δn in z are increasingly dominant, as they arise from the increasingly larger widths of the disorder spectra: $\delta k\approx 0.13$ and $0.71\,\mu\mathrm{m}^{-1}$, leading to a characteristic distance of variations of $z_0\approx 1.023$ and 0.608 mm, respectively. The cross-sections shown in Fig. 2c,d, taken through the ensemble-averaged beam, show an increasing deviation from the exponential structure characterizing the Anderson-localized beam of Fig. 2b. However, an even more important fact is apparent from the widths of the (ensemble-averaged) beams experiencing dynamic disorder: their widths, $\sim$230 μm and $\sim$270 μm (with standard deviations 15 μm and 10.5 μm), are much larger than the width of the freely diffracting beam ($\sim$166 μm) of Fig. 2a. That is, the beams propagating through the rapidly fluctuating spatial disorder exhibit hyper-transport: the wave packets expand much faster than ballistic expansion.

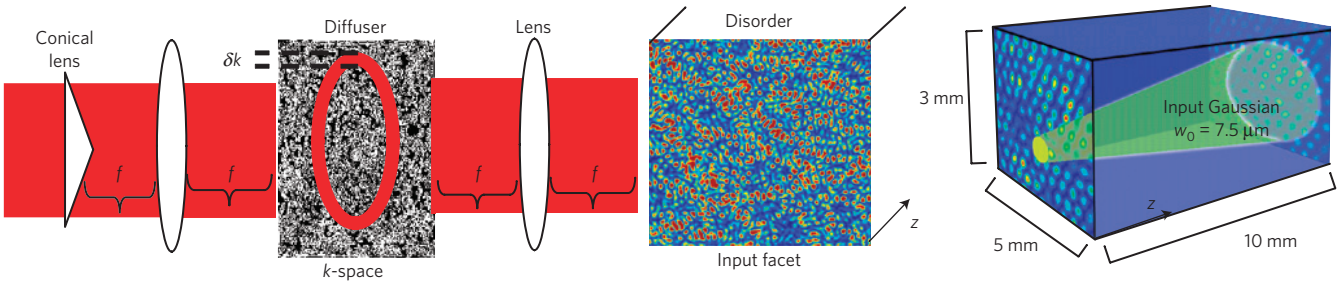

Figure 1 | Experimental scheme for studying hyper-transport of light by virtue of evolving disorder. Left panel: making the dynamically evolving disorder. A wide Gaussian beam is passed through a conical lens, which generates a ring of light of width δk at a predetermined plane. A diffuser placed at this plane introduces a phase that varies randomly from point to point on the ring. The ring of light and the random phase superimposed on it form the Fourier spectrum of the disorder. A spherical lens transforms this spectrum into a speckled beam that is propagating through a photosensitive material where it induces a change in the refractive index proportional to the intensity pattern. The refractive index change is disordered in the x–y plane, whereas its rate of variation in z is proportional to $1/\delta k$. Right panel: a weak probe is launched into the disordered dielectric medium, and monitored at the output facet.

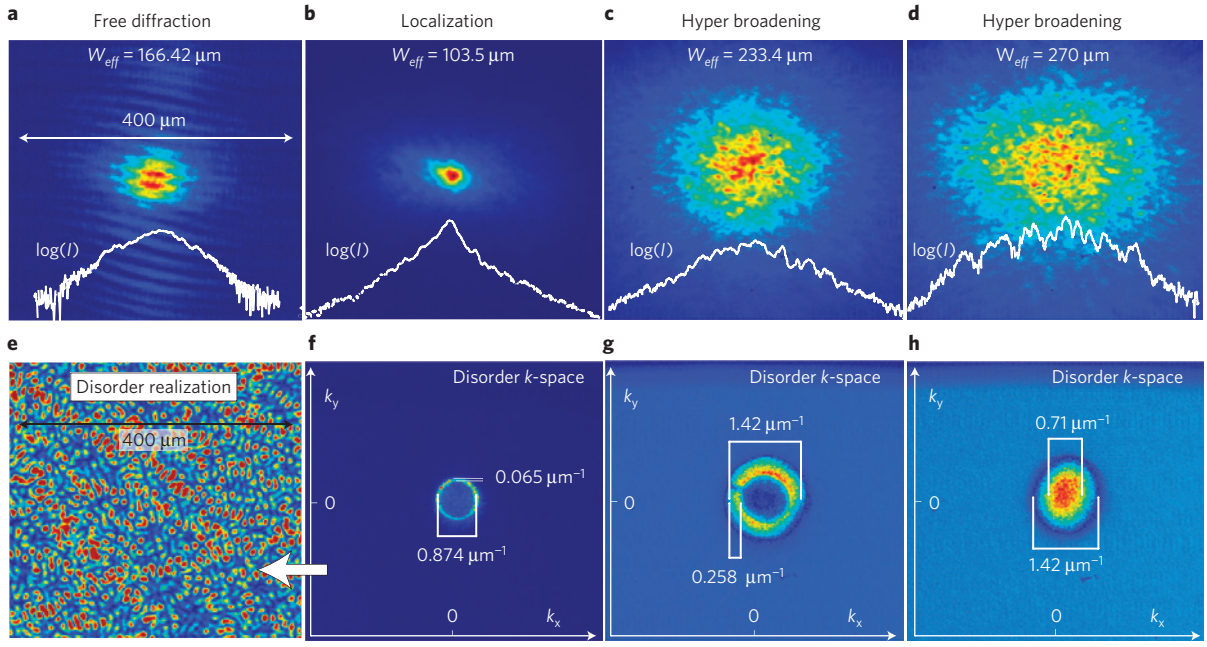

Figure 2 | Experiments demonstrating hyper-transport of light, by controlling the evolution rate of spatial disorder. a–**d**, Ensemble-averaged intensity, I, structure of the beam exiting the disordered medium. The cross-sections shown therein are shown in a logarithmic scale, with their corresponding width W_{eff}. In all of these experiments, the input beam is a Gaussian beam of 524 nm wavelength and an initial width of ~15 μm full-width at half-maximum. It is propagating through the disordered medium for 1 cm. **a**, When the medium is homogeneous, the freely diffracting beam broadens to 166.42 μm. **b**, When the disorder is propagation-invariant, the beam exhibits Anderson localization, manifested in its exponential structure. **c**,**d**, When the disorder evolves during propagation, the beam expands faster than ballistic expansion (hyper-transport). **e**–**h**, Various realizations of the disorder. **e**, One typical realization of the speckled structure inducing the disordered refractive index structure whose Fourier spectrum in shown in **f**. In this case, the Fourier spectrum is a very thin ring; hence, the disorder is propagation-invariant, causing Anderson localization as shown in **b**. **g**,**h**, Fourier spectra of the evolving disorder leading to hyper-transport. In this case, the spectrum corresponds to a thick ring (**g**) or a full circle (**h**), inducing evolving disorder, and leading to hyper-transport. Indeed, the widths of the ensemble-averaged exit beams with such disorder are much broader (**c**,**d**) than the width of the freely diffracting beam shown in **a**.

We corroborate these experimental findings with the simulations shown in Fig. 3. Figure 3a shows the simulated freely diffracting beam of an initial width of ~15 μm broadening to a width similar to that of Fig. 2a. Figure 3b shows the ensemble-averaged (over 50 realizations of disorder) intensity pattern and width of the same initial wave packet, after propagating in the presence of dynamic disorder whose (plane wave) spectrum is numerically constructed from the experimental spectrum shown in Fig. 2h. The value of the beam width (240 μm with standard deviation of 11 μm) and the log-plot cross-section of the intensity structure shown in Fig. 3b are similar (within 10% deviation) to the experimental results shown in Fig. 2d, both exhibiting hyper-transport. Clearly, the simulated results agree very well with the experiments.

These experimental and numerical findings raise fundamental questions on the evolution of the spectrum of wave packets undergoing hyper-transport. For ballistic expansion (free propagation), the power spectrum is conserved, as the expansion occurs only because different spectral constituents (of the plane-wave spectrum, in our case) accumulate phase at different rates. Likewise, the power spectrum of a wave packet undergoing Anderson localization is found to expand initially (as it scatters from the disorder) until localization is reached, but then the spectral expansion is found to stop, and the power spectrum is conserved on further

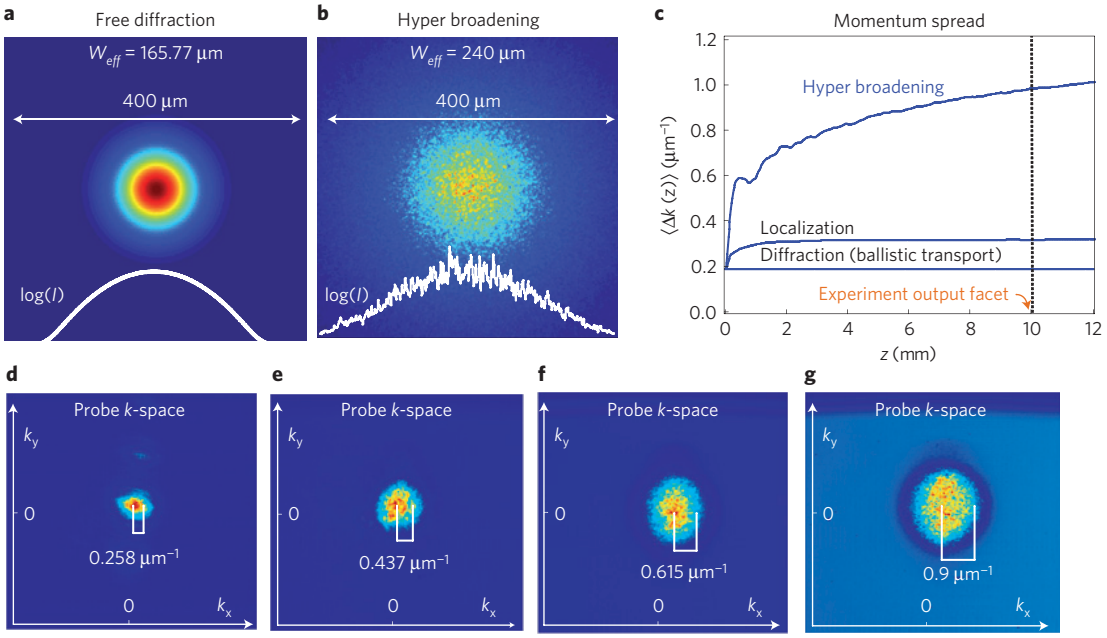

Figure 3 | Experiments and simulations showing the evolution of the momentum power spectrum of the wave packet propagating through the disordered photonic medium. a–c, Simulations. **a**, Intensity structure and beam width of the freely diffracting beam exiting a homogeneous medium after 1 cm of propagation, for an initial beam width of ~15 μm. **b**, Ensemble-averaged intensity pattern and width for the same input beam, after propagating in the dynamically evolving spatial disorder. The spectrum of the disorder in **b** is constructed from the Fourier spectrum measured in the experiments of Fig. 2h. Note the agreement between the simulated results (**b**) and experiments (Fig. 2d). **c**, Simulated evolution of the width of the Fourier spectra of the beams, undergoing ballistic transport (homogeneous medium; lower curve), localization (propagation-invariant disorder; middle curve), and hyper-transport (evolving disorder; upper curve). For ballistic transport the spectral width is conserved, whereas for localization the spectrum initially expands, but once localization is reached, the mean spectral width remains unchanged. In contrast to that, the spectrum of a beam undergoing hyper-transport is continuously expanding. **d–g**, Experiments. **d–g**, The corresponding experimental results showing the optical spatial power spectrum of the exiting beam whose real-space intensity pattern is presented in Fig. 2a–d, respectively.

propagation (for related references, see refs 8,32–34). Certainly, to understand the results shown in Fig. 2c,d, it is important to examine what happens to the power spectrum of a wave packet undergoing hyper-transport.

Recalling that (k_x, k_y) are equivalent to the momentum in the Schrödinger equation, we simulate the propagation of the beam through the disordered medium and calculate the spatial spectrum spread $\Delta k_\perp$ as function of z, for the cases of free diffraction, Anderson localization and hyper-transport. For each realization of the disorder, we calculate $\Delta k_\perp(z)$, by treating the momentum representation of the wave packet—$|\Psi(k_x,k_y,z)|^2 = |\int \Psi(x,y,z)\cdot e^{-ik_x x}\cdot e^{-ik_y y}\,dx\,dy|^2$—as the probability density. We then average our results over an ensemble of different realizations of the disorder, and show them in Fig. 3c. The corresponding experimental results are shown in Fig. 3d–g. These figures (taken from the output facet of the disordered medium) show the optical power spectrum (absolute value squared of the Fourier transform) of the wave packet whose real-space intensity pattern is presented in Fig. 2a–d, respectively. Experimentally, the spatial power spectrum is monitored by passing the beam exiting the medium ($z = 10$ mm) through a lens and capturing the intensity pattern at the focal plane with a camera. Let us now examine the results. In the case of the free diffraction, Fig. 3d shows the spatial power spectrum of the beam in Fig. 2a. Indeed, the power spectrum of this freely diffracting beam is the same as the power spectrum of the input beam, as is always the case for ballistic transport in a homogeneous system. The simulations presented in Fig. 3c highlight this feature: $\Delta k_\perp$ in the case of free diffraction does not change during propagation. Consider now the case where the beam is propagating through z-invariant disorder, where the beam becomes localized (Fig. 2b). The power spectrum of this localized beam is shown in Fig. 3e: the spectral width $\Delta k_\perp$ of the localized beam is wider than the initial spectral width (compare Fig. 3e with Fig. 3d). Simulations of this case, presented in Fig. 3c, reveal that $\Delta k_\perp$ grows during the early stages of propagation, where the ensemble-averaged beam reshapes owing to multiple scattering, but after localization is reached, the (ensemble-averaged) spectral width seems to remain unchanged. Finally and most interestingly, in contrast to the propagation-invariant power spectra of wave packets undergoing ballistic transport and of (ensemble-average) wave packets in the Anderson-localized state, we find that the power spectrum of beams undergoing hyper-transport is always broadening (expanding) throughout propagation (see Fig. 3f,g).

Before closing, we discuss the main aspects of hyper-transport, propose some intuitive understanding and raise open questions. We shall do this through the view point of the Schrödinger equation, while relating to our photonic picture as reflected in the experiments. On the one hand, the temporally fluctuating potential evolves in a random fashion; hence, it cannot support continuous acceleration or deceleration for any particular part of the wave packet. On the other hand, the spectral expansion measured during hyper-transport clearly implies acceleration, which means that kinetic energy is being deposited into the system. This is indeed manifested in the higher velocities and spectral expansion observed in our experiments and simulations. A natural question to ask is: for how long would the spectral expansion and the hyper-transport persist? When the spectrum of the disorder is unbound, the expansion could continue indefinitely, because momentum can be continuously transferred from ever higher spectral components of the disorder to the wave packet, continuously expanding its spectrum and supporting its ongoing hyper-transport in real space. Most probably, such ongoing expansion will exhibit universal exponents. A more interesting question is: what would happen if the

spectrum of the disorder is finite, as it is in any physical system and of course in our system (Fig. 2f–h)? The answers to these questions call for future research, but we can already foresee two distinct regimes where the physics may be entirely different. To explain the intuition, we recall the analogy between our optical system and a quantum particle under the influence of a time-varying potential.

The first regime of hyper-transport occurs when the z-variation of the disorder is sufficiently slow. In optical systems such as ours, this regime corresponds to spectral components of the wave packet undergoing consecutive Bragg scattering off the multiple gratings comprising the spatial disorder. When scattering from a specific grating, momentum is exchanged between the wave packet and the disorder. However, for monochromatic light, each plane-wave component comprising the wave packet is Bragg-matched to scatter from a single spectral component of the disorder, and is therefore scattered into a single direction determined by momentum conservation. Each scattering event can extract only one quantum of momentum from the disorder. The presence of multiple consecutive Bragg scattering events makes the momentum spectrum of the wave packet grow, as we observe in Fig. 3. To be in this Bragg regime, the rate of evolution of the disorder must be sufficiently slow to enforce phase-matching (momentum conservation) in each scattering event. All of the experiments and simulations presented in this article are in this Bragg regime. Under rather general conditions (sufficiently high momentum), it is generally believed that such a problem can be described by classical dynamics. In this context, one-dimensional hyper-transport seems to be a transient phenomenon, and would eventually stop at some point after which the wave-packet expansion will continue at a ballistic rate[35,36].

The second regime of hyper-transport occurs when the disorder evolves very fast. In our optical system, this regime corresponds to the case where the z-component of the momentum mismatch between the incident and scattered waves times the characteristic distance for disorder evolution, z_0, is much smaller than π. This is the regime of thin holograms, often referred to as the Raman–Nath regime[37,38], where a wave can scatter from many momentum components of the disorder simultaneously (not only from a single component, as in the Bragg regime). The quantum analogue would be of an electron excited from one energy level to another by an electromagnetic field that is oscillating only for a very short time, around a frequency detuned from the difference between the energy levels. In this case the probability of the transition is non-vanishing. Returning to our optical system, could we expect that spectral broadening and hyper-transport will persist in this regime even when the spectral width of the wave packet is much broader than that of the disorder? We leave this intriguing question for future research. If this regime is indeed physical, this would be a very rare example where the high-energy dynamics of waves fundamentally differs from the classical dynamics of particles: a violation of the correspondence principle.

Throughout this article we described the system in universal terms, not specific to electromagnetic waves, as manifested by the analogy between the Schrödinger equation and the paraxial wave equation. As such, hyper-transport is in fact a universal concept, which should be observable in a variety of systems beyond optics, such as matter waves, sound waves, plasma, and in the transport of conduction electrons in semiconductors. Furthermore, fundamentally, once such temporal acceleration would reach very high velocities, relativistic effects would have to be included. Most certainly, these ideas open a range of exciting possibilities. However, the dynamics of electromagnetic waves is actually very rich in its own right. For example, how would optical nonlinearities affect hyper-transport? Furthermore, in view of the recent experiments on quantum walks of correlated photons[39] and on localization with entangled photons[40], it would be extremely interesting to know whether the phenomenon of hyper-transport would occur also with entangled photons. These and many other questions are left for future research. Our article has presented the first experimental observation of hyper-transport, opening a new research direction that is universal for all wave systems containing disorder. At same time, the underlying ideas certainly hold further aspects unique to the specific waves propagating in the disordered system.

Received 6 June 2012; accepted 19 September 2012; published online 11 November 2012

References

1. Anderson, P. W. Absence of diffusion in certain random lattices. *Phys. Rev.* **109,** 1492–1505 (1958).
2. Lee, P. A. & Ramakrishnan, T. V. Disordered electronic systems. *Rev. Mod. Phys.* **57,** 287–337 (1985).
3. Schwartz, T., Bartal, G., Fishman, S. & Segev, M. Transport and Anderson localization in disordered two-dimensional photonic lattices. *Nature* **446,** 52–55 (2007).
4. Lahini, Y. *et al.* Anderson localization and nonlinearity in one-dimensional disordered photonic lattices. *Phys. Rev. Lett.* **100,** 013906 (2008).
5. Wiersma, D. S., Bartolini, P., Lagendijk, A. & Righini, R. Localization of light in a disordered medium. *Nature* **390,** 671–673 (1997).
6. Chabanov, A. A., Stoytchev, M. & Genack, A. Z. Statistical signatures of photon localization. *Nature* **404,** 850–853 (2000).
7. Störzer, M., Gross, P., Aegerter, C. M. & Maret, G. Observation of the critical regime near Anderson localization of light. *Phys. Rev. Lett.* **96,** 063904 (2006).
8. Billy, J. *et al.* Direct observation of Anderson localization of matter waves in a controlled disorder. *Nature* **453,** 891–894 (2008).
9. Giacomo, R. *et al.* Anderson localization of a non-interacting Bose–Einstein condensate. *Nature* **453,** 895–898 (2008).
10. Kondov, S. S., McGehee, W. R., Zirbel, J. J. & DeMarco, B. Three-dimensional Anderson localization of ultracold matter. *Science* **334,** 66–68 (2011).
11. Jendrzejewski, F. *et al.* Three dimensional localization of ultracold atoms in an optical trap. *Nature Phys.* **8,** 398–403 (2012).
12. Hu, H., Strybulevych, A., Page, J. H., Skipetrov, S. E. & van Tiggelen, B. A. Localization of ultrasound in a three dimensional elastic network. *Nature Phys.* **4,** 945–948 (2008).
13. Kampen, N. V. *Stochastic Processes in Physics and Chemistry* 3rd edn (North Holland, 2007).
14. Zaslavskii, G. M. & Chirikov, B. V. Stochastic instability of nonlinear oscillation. *Sov. Phys. Usp.* **14,** 549–567 (1972).
15. Jayannavar, A. M. & Kumar, N. Nondiffusive quantum transport in a dynamically disordered medium. *Phys. Rev. Lett.* **48,** 553–556 (1982).
16. Golubovic, L., Feng, S. & Zeng, F. Classical and quantum superdiffusion in a time-dependent random potential. *Phys. Rev. Lett.* **67,** 2115–2118 (1991).
17. Rosenbluth, M. N. Comment on Classical and quantum superdiffusion in a time-dependent random potential. *Phys. Rev. Lett.* **69,** 1831–1831 (1992).
18. Arvedson, E., Wilkinson, M., Mehlig, B. & Nakamura, K. Staggered ladder spectra. *Phys. Rev. Lett.* **96,** 030601 (2006).
19. De Raedt, H., Lagendijk, A. & de Vries, P. Transverse localization of light. *Phys. Rev. Lett.* **62,** 47–50 (1988).
20. Longhi, S. Quantum-optical analogies using photonic structures. *Laser Photon. Rev.* **3,** 243–261 (2009).
21. Lederer, F. *et al.* Discrete solitons in optics. *Phys. Rep.* **463,** 1–126 (2008).
22. Martin, L. *et al.* Anderson localization in optical waveguide arrays with off-diagonal coupling disorder. *Opt. Express* **19,** 13636–13646 (2011).
23. Lahini, Y. *et al.* Observation of a localization transition in quasiperiodic photonic lattices. *Phys. Rev. Lett.* **103,** 013901 (2009).
24. Levi, L. *et al.* Disorder-enhanced transport in photonic quasicrystals. *Science* **332,** 1541–1544 (2011).
25. Szameit, A. *et al.* Wave localization at the boundary of disordered photonic lattices. *Opt. Lett.* **35,** 1172–1174 (2010).
26. Barthelemy, P., Bertolotti, J. & Wiersma, D. S. A Lévy flight for light. *Nature* **453,** 495–498 (2008).
27. Zhang, S., Park, J., Milner, V. & Genack, A. Z. Photon delocalization transition in dimensional crossover in layered media. *Phys. Rev. Lett.* **101,** 183901 (2008).
28. Efremidis, N. K., Sears, S. & Christodoulides, D. N. Discrete solitons in photorefractive optically induced photonic lattices. *Phys. Rev. E* **66,** 046602 (2002).
29. Fleischer, J. W., Carmon, T., Segev, M., Efremidis, N. K. & Christodoulides, D. N. Observation of discrete solitons in optically induced real time waveguide arrays. *Phys. Rev. Lett.* **90,** 023902 (2003).
30. Fleischer, J. W., Segev, M., Efremidis, N. K. & Christodoulides, D. N. Observation of two-dimensional discrete solitons in optically induced nonlinear photonic lattices. *Nature* **422,** 147–150 (2003).

31. Segev, M., Valley, G. C., Crosignani, B., DiPorto, P. & Yariv, A. Steady-state spatial screening solitons in photorefractive materials with external applied field. *Phys. Rev. Lett.* **73,** 3211–3214 (1994).
32. Gurevich, E. & Kenneth, O. Lyapunov exponent for the laser speckle potential: A weak disorder expansion. *Phys. Rev. A* **79,** 063617 (2009).
33. Lugan, P. *et al.* One-dimensional Anderson localization in certain correlated random potentials. *Phys. Rev. A* **80,** 023605 (2009).
34. Shapiro, B. Cold atoms in the presence of disorder. *J. Phys. A* **45,** 143001 (2012).
35. Krivolapov, Y., Levi, L., Fishman, S., Segev, M. & Wilkinson, M. Super-diffusion in optical realizations of Anderson localization. *New J. Phys.* **14,** 043047 (2012).
36. Krivolapov, Y. & Fishman, S. Universality classes of transport in time-dependent random potentials. *Phys. Rev. E* **86,** 030103 (2012).
37. Saleh, B.E.A. & Teich, M.C. *Fundamentals of Photonics* Ch. 20 (Wiley, 1991).
38. Moharam, M. G. & Young, L. Criterion for Bragg and Raman-Nath diffraction regimes. *Appl. Opt.* **17,** 1757–1759 (1978).
39. Peruzzo, A. *et al.* Quantum walks of correlated photons. *Science* **329,** 1500–1503 (2010).
40. Abouraddy, A. F., Di Guiseppe, G., Christodoulides, D. N. & Saleh, B. E. A. Anderson localization and co-localization of spatially entangled photons. *Phys. Rev. A* **86,** 040302 (2012).

Acknowledgements

This research was supported by an Advanced Grant from the European Research Council, by the Israel Science Foundation and by the USA–Israel Binational Science Foundation.

Author contributions

The experiments were carried out by L.L. All authors contributed to this research.

Additional information

Reprints and permissions information is available online at www.nature.com/reprints. Correspondence and requests for materials should be addressed to M.S.

Competing financial interests

The authors declare no competing financial interests.